ELSEVIER

Journal of Nuclear Materials 258–263 (1998) 1848–1855

journal of nuclear materials

Electrical conductivity and current-voltage characteristics of alumina with or without neutron and electron irradiation

K. Shiiyama [a,*], M.M.R. Howlader [a], S.J. Zinkle [b], T. Shikama [c], M. Kutsuwada [a], S. Matsumura [a], C. Kinoshita [a]

[a] *Department of Nuclear Engineering, Kyushu University, Hakozaki, Higashi-ku, Fukuoka 812-8581, Japan*
[b] *Metals and Ceramics Division, Oak Ridge National Laboratory, P.O. Box 2008, Oak Ridge, TN 37831-6376, USA*
[c] *The Oarai Branch, IMR, Tohoku University, Oarai, Higashiibarakigun, Ibarakiken 311-1313, Japan*

Abstract

The in situ measurement of electrical conductivity and of current–voltage (*I–V*) characteristics of single- and polycrystal alumina have been carried out both in HFIR (high flux isotope reactor; Oak Ridge National Laboratory) at 723 K with or without neutron irradiation and in a High Voltage Electron Microscope (HVEM) from room temperature to 723 K with or without 1 MeV electron irradiation. Radiation induced conductivity (RIC) was observed for all specimens under neutron and electron irradiation. The RIC under electron irradiation increased with increasing electron flux. There was no catastrophic bulk or surface conductivity degradation under neutron and electron irradiation up to >2 dpa and 9.1×10^{-5} dpa, respectively. Non-ohmic *I–V* behavior was observed for all specimens with or without neutron and electron irradiation. The *I–V* behavior with irradiation was similar to that without irradiation. The reason for non-ohmic behavior is discussed on the basis of the difference of work function between electrode and specimen materials. © 1998 Elsevier Science B.V. All rights reserved.

1. Introduction

Alumina is one of the leading candidates for insulator and radiofrequency window/feedthrough applications in magnetic fusion reactors [1,2]. For insulator applications it is necessary to understand the basic electrical properties of alumina. Radiation induced conductivity (RIC) and radiation induced electrical degradation (RIED) of alumina under irradiation are two of the critical issues for its application to fusion reactors. Many results for RIC show that RIC is not severe for insulators in International Thermal Reactor (ITER) [3,4]. Although RIED studies have been performed by many researchers, these studies used widely varying irradiation conditions (electrons [5–8], ions [9–11] and neutrons [12–14]) and different grades of alumina. Moreover, some researchers observed RIED and the others did not. Thus the RIED phenomenon became controversial [4,15]. The in situ measurements of several kinds of alumina under identical irradiation conditions are needed to resolve the controversial results on RIED.

The current–voltage (*I–V*) behavior is one of the important basic electrical properties that can provide insight into the phenomena responsible for ohmic or non-ohmic behavior of semiconductors and insulators. For example, the mechanism of electrical conductivity may be obtained from an analysis of the *I–V* characteristic behavior. Although many studies have been performed on the electrical conductivity of alumina, there are few reports of *I–V* measurement with or without irradiation [14].

The objective of the present study is to investigate the physical mechanisms responsible for the electrical conductivity and *I–V* behavior of alumina by performing in situ electrical measurements on alumina with or without neutron and electron irradiation.

---

[*] Corresponding author. Tel.: +81-92 642 3773; fax: +81-92 642 3771; e-mail: kstne@mbox.nc.kyushu-u.ac.jp.

0022-3115/98/$19.00 © 1998 Elsevier Science B.V. All rights reserved.
PII: S0022-3115(98)00339-0

2. Experimental procedure

2.1. Neutron irradiation

Twelve grades of single- and poly-crystal alumina specimens were used in the neutron irradiation study. The vendor and grade of specimens is shown in Table 1. The size of all specimens was 8 mm in diameter and 0.75 mm in thick. A total of 15 specimens were irradiated at 723 K with or without electric field of 200 kV/m in the High Flux Isotope Reactor (HFIR) at Oak Ridge National Laboratory (ORNL). The full power reactor ionizing dose rate was 10–16 kGy/s and the average displacement damage rate was ~ 2.4–4.3×10^{-7} dpa/s. The guard and center electrodes were made of a titanium ($\leqslant 0.1$ μm) underlayer and platinum (~ 1 μm) overlayer by vapor deposition in vacuum. Each specimen was put into a subcapsule and 15 subcapsules were inserted into the irradiation capsule. The detailed subcapsule and capsule design were described elsewhere [16]. In situ measurement of electrical conductivity and *I–V* measurements were performed by using a Keithley 237 Source Measure Unit and two Keithley 6517 electrometers. A mineral insulated (MI) coaxial cable was used as the power lead, and a triaxial MI cable was used as the data lead from the guard and center electrodes for each subcapsule.

2.2. Electron irradiation

Single crystal alumina (Kyocera SA-100, 99.99% purity) was used for the electron irradiation study. The size of the specimen was 5.5 mm in diameter and 0.75 mm thick. The guard and center electrodes were made from vapor-deposited titanium (<0.1 μm) and gold (~ 1 μm) layers. The specimen holder was specifically designed for in situ measurement of electrical conductivity in a high voltage electron microscope (HVEM), and *I–V* measurements were performed at the temperature range from 293 to 723 K with or without electron irradiation. The details of the specimen holder were described previously [17]. Irradiation with 1 MeV electrons flux of 1.5×10^{18} e/m^{2}s (9.3×10^4 Gy/s and 1.7×10^{-4} dpa/s) was performed with an HVEM in the Research Laboratory for High Voltage Electron Microscopy, Kyushu University. A Hewlett Packard HP4339A high resistance meter was used both to apply voltage to specimen and to measure the specimen current.

3. Results

3.1. Neutron irradiation

Fig. 1 shows the irradiation time dependence of the current in a Crystal Systems single crystal alumina (Hemex) regular grade specimen. The irradiation of 2500 h corresponded to a dose of ~ 2.2 dpa (displacements per atom) for this specimen position in the HFIR capsule. The current increased quickly after the reactor start and reached a maximum value, then decreased gradually. When the reactor stopped, the current decreased to the preirradiation value. Thus the increase of current is considered to be RIC rather than RIED. It is seen in Fig. 1 that there is no drastic increase of current

Table 1
Specimen list for the in situ measurement of electrical conductivity in HFIR

HFIR position	Material, vendor and grade	Applied voltage (V)	Total dose RIED
1	Al_2O_3, single crystal, Crystal Systems (Hemex UV grade) *a*-axis	150	(0.07 dpa) [a], (shorted coax)
2	Al_2O_3, single crystal, Crystal Systems (Hemex UV grade) *c*-axis	150	2 dpa, no RIED
3	Al_2O_3, single crystal, Crystal Systems (Hemex regular) *c*-axis	150	2.2 dpa, no RIED
4	Al_2O_3, single crystal, Crystal Systems (Hemex regular) *a*-axis	150	(0.2 dpa) [a], (open coax)
5	Al_2O_3, polycrystalline, Vitox (99.9% purity)	150	(0.07 dpa) [a] , (shorted coax)
6	Al_2O_3, polycrystalline, Kyocera A-480 (99.9% purity)	150	(0.006 dpa) [a], (Shorted coax)
7	Al_2O_3, polycrystalline, Wesgo AL300 (97.0% purity)	150	(1 dpa) [a], no RIED, shorted coax
8	Al_2O_3, polycrystalline, Kyocera A-479 (99.0% purity)	150	(1 dpa) [a], no RIED, shorted coax
9	Al_2O_3, polycrystalline, Coors AD998 (99.8% purity)	150	(0.005 dpa) [a], open triax
10	Al_2O_3, polycrystalline, Wesgo AL995 (99.5% purity)	150	(0.03 dpa) [a], shorted coax
11	Al_2O_3, polycrystalline, Wesgo AL995 (99.5% purity)	0	(2 dpa) [a], no RIED, open triax
12	Al_2O_3, single crystal, Crystal Systems (Hemex regular) *c*-axis	0	(0.5 dpa) [a], shorted coax
13	Al_2O_3+Cr, single crystal, Union Carbide (UV grade), 60□ from *c*-axis	150	2 dpa no RIED
14	Al_2O_3, single crystal, Kyocera SA100 (1102 orientation)	150	(0.02 dpa) [a], shorted coax
15	Al_2O_3, single crystal, Kyocera SA100 (1102 orientation)	0	(0.3) dpa) [a], shorted coax

[a] MI cable failed (short or open) during the full power irradiation.

besides the normal RIC up to dose of ∼2.2 dpa. The results for the in situ measurements are summarized in the fourth column in Table 1. The in situ measurements could be performed up to three HFIR irradiation cycles (maximum dose of ∼3 dpa) for only three specimens: single crystal of Crystal Systems (Hemex) *c*-axis direction, regular and UV grade, and Cr doped single crystal of Union Carbide (UV grade). The measurements on other specimens were prematurely terminated because the coaxial or triaxial MI cable either shorted or developed an open circuit during the 3-month neutron irradiation. However, measurements on three of these specimens (Wesgo AL300, Kyocera A-479 and Wesgo AL995) were performed for doses up to 1 or 2 dpa. Furthermore, the results on three specimens (Crystal Systems UV and regular grade single crystal alumina and Union Carbide Cr-doped UV grade single crystal alumina) also show that there was no drastic increase of current for doses up to >2 dpa. Thus it is concluded that there is no catastrophic levels of RIED in alumina up to >2 dpa for neutron irradiation at ∼723 K for electric field strengths of ∼200 V/mm. Further experimental results are given elsewhere [18].

Figs. 2 and 3 show the *I–V* characteristics of a Crystal Systems (Hemex) UV grade single crystal alumina specimen without and with neutron irradiation, respectively. The curves of *I–V* plots are not linear, that is, the *I–V* characteristics are non-ohmic. Moreover the curves are asymmetric. The magnitude of the current at the same absolute value of applied voltage is greater for positive voltages than for negative voltages. Non-ohmic *I–V* characteristics were observed for all of the specimens with the reactor turned off. The *I–V* characteristics were also non-ohmic during reactor irradiation, but the characteristics were quantitatively different from those without reactor irradiation. The qualitative in situ *I–V* characteristics were similar between specimens measured with the reactor on and off (non-ohmic behavior, with higher current flow observed at positive voltages in all cases).

3.2. Electron irradiation

The fluence dependence of the bulk and surface conductivity is shown in Fig. 4. The bulk and surface conductivity was measured simultaneously. The con-

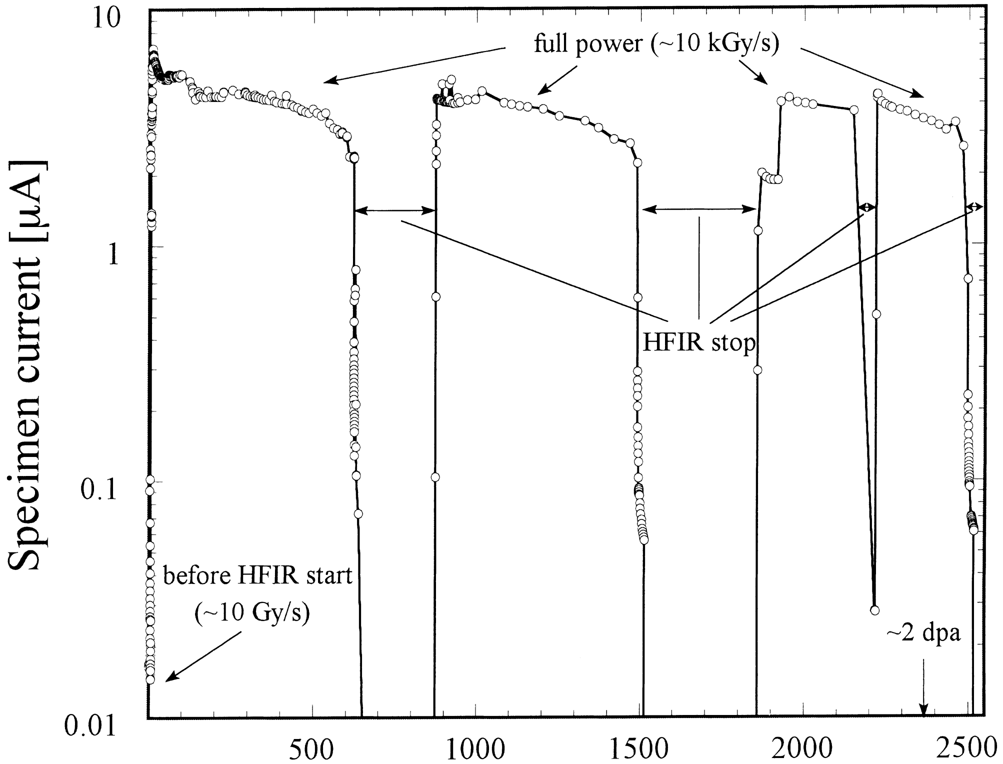

Fig. 1. Irradiation time dependence of current of Crystal Systems "Hemex" UV grade *c*-axis single crystal alumina under HFIR irradiation. The irradiation of 2500 h corresponds to a dose of ∼2.2 dpa.

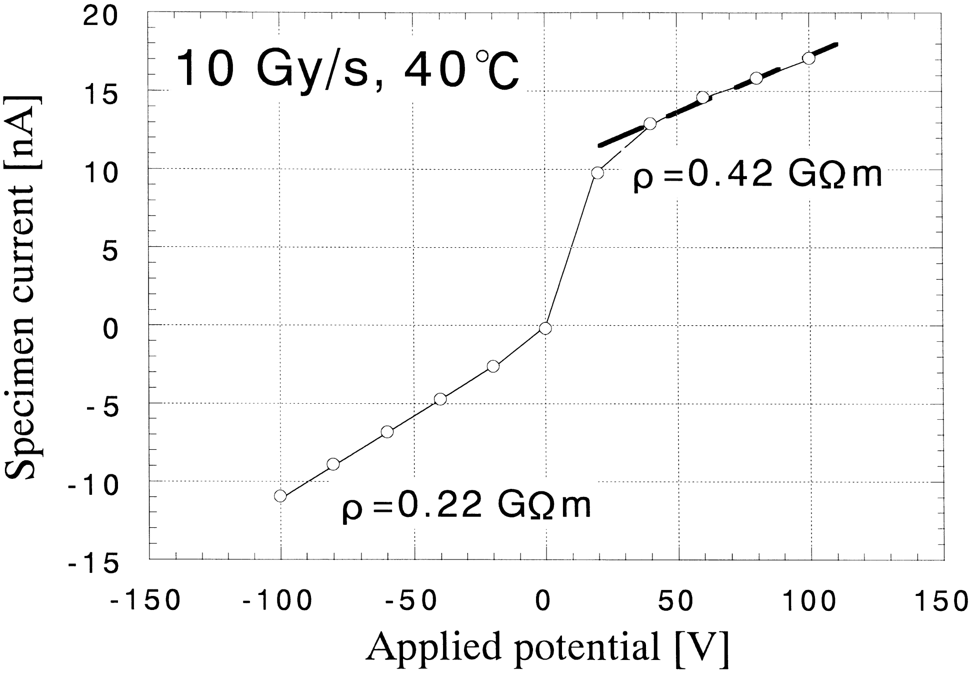

Fig. 2. Current–voltage plot of Crystal Systems "Hemex" UV grade *c*-axis single crystal alumina without neutron irradiation at 313 K.

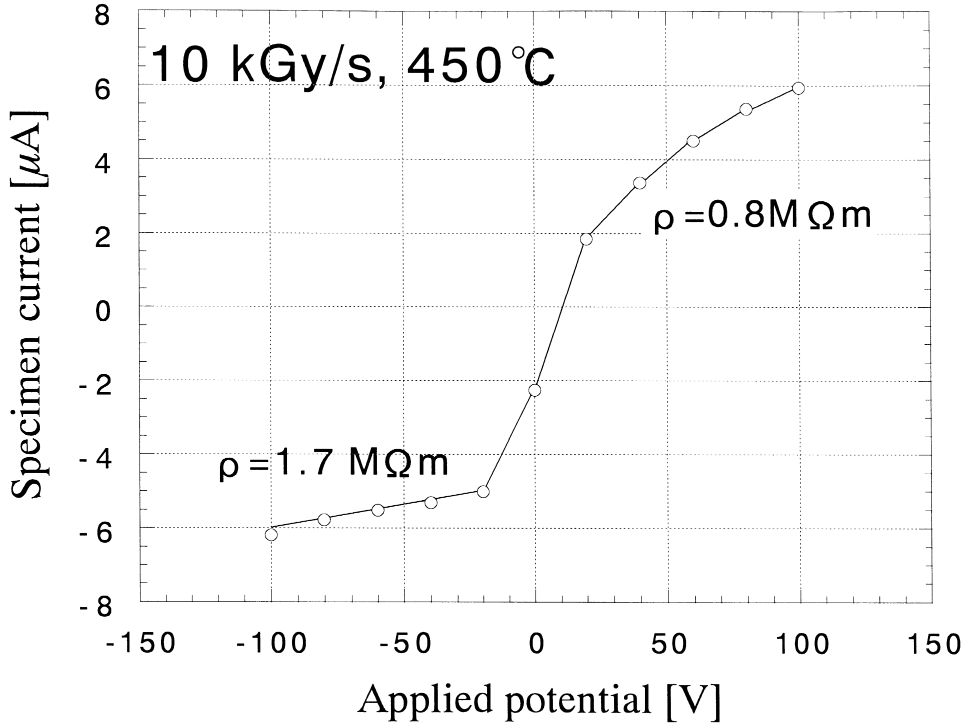

Fig. 3. Current–voltage plot of Crystal Systems "Hemex" UV grade *c*-axis single crystal alumina with neutron irradiation at 723 K.

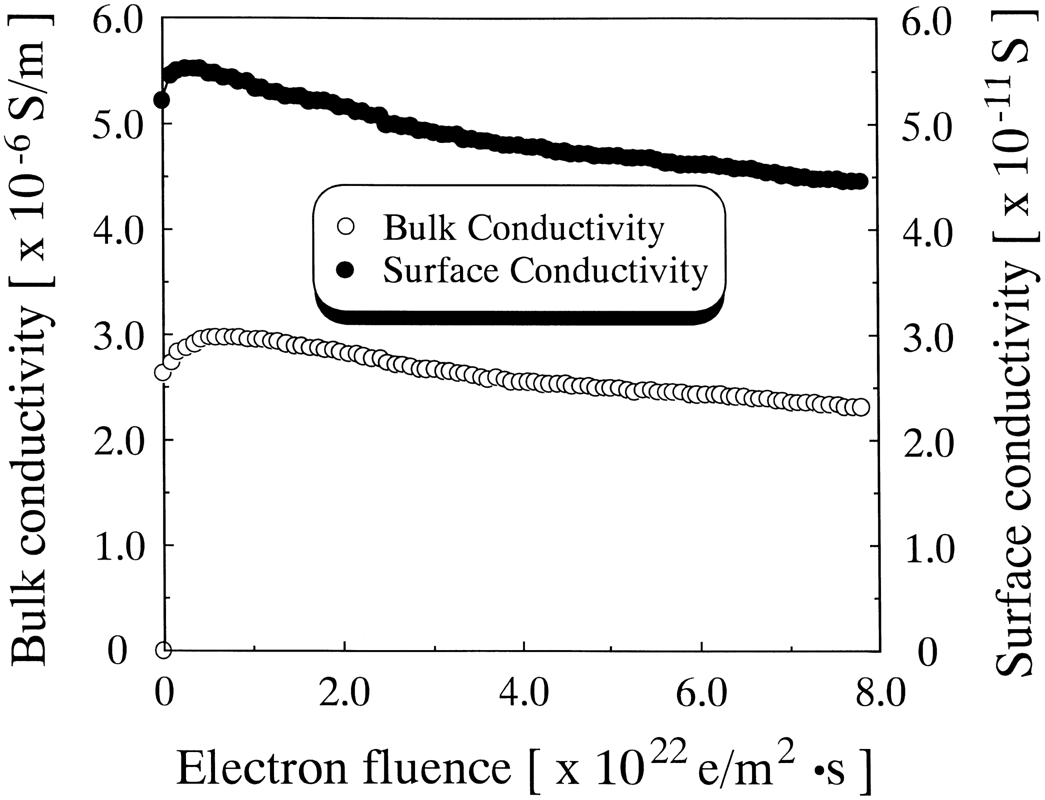

Fig. 4. Electron fluence dependence of bulk (open circle) and surface (filled circle) conductivity of Kyocera "SA-100" single crystal alumina under 1 MeV electron irradiation flux of 1.4×10^{18} e/m^{2}s with an electric field of 93 kV/m at 680 K. The scale of bulk conductivity is different from that of surface conductivity.

ductivity was measured under irradiation with a 1 MeV electron flux of 1.4×10^{18} e/m^{2}s in an electric field of 93 kV/m at 680 K. The bulk and surface conductivity increased to a maximum value (3.0×10^{-6} S/m for bulk and 5.6×10^{-11} S for surface at 0.5×10^{22} e/m^2) then decreased gradually up to a fluence of 7.8×10^{22} e/m^2 (9.1×10^{-5} dpa). The fluence dependence of the surface conductivity is similar to that of bulk conductivity. The results show that there is no pronounced degradation of bulk and surface conductivity up to 9.1×10^{-5} dpa.

Fig. 5 shows the *I–V* behavior before irradiation from room temperature to 723 K. In Fig. 5, solid and dotted lines show the increasing and decreasing voltage process, respectively. It was found that the *I–V* behavior had a strong temperature dependence. The activation energy obtained from the temperature dependence was 0.4 ± 0.02 eV. The *I–V* behavior is non-ohmic and the *I–V* curve is asymmetric. The *I–V* curve at 723 K has hysteresis. The *I–V* behavior under irradiation with a 1 MeV electron flux of 1.5×10^{18} e/m^{2}s is shown in Fig. 6. Non-ohmic behavior was also observed but the behavior was different from the non-irradiated case. The *I–V* behavior under irradiation has less temperature dependence compared with that of without irradiation. The activation energy obtained from the temperature dependence was 0.09 ± 0.04 eV.

4. Discussion

Non-ohmic *I–V* behavior in semiconductor materials is usually considered to be mainly due to the difference between the work function of the electrode and the electron affinity of the specimen. In the case of a semiconductor specimen, an ohmic contact can be obtained by choosing an electrode with a smaller work function than the electron affinity of the specimen if it is an n-type semiconductor (or a larger work function if p-type) [19]. The electron affinity of alumina and the work function of titanium are 1 eV [20] and 4.33 eV [21], respectively. If the work function concept for semiconductors could be applied to alumina, the non-ohmic *I–V* characteristics observed for the alumina specimens with titanium electrodes is evidence that alumina behaves as an n-type semiconductor. RIC studies on alumina have concluded that the electron mobility is much higher than the hole

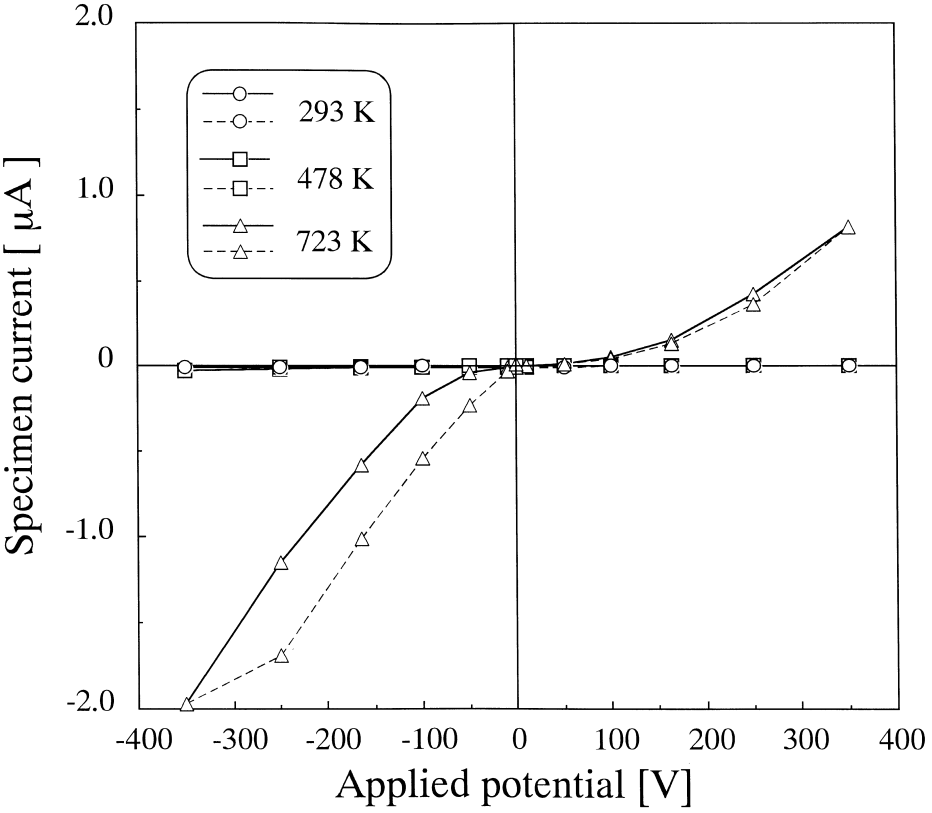

Fig. 5. Current–voltage plot of Kyocera "SA-100" single crystal alumina without electron irradiation at various temperatures. Solid and dotted lines correspond to the increasing and decreasing voltage process, respectively.

mobility [22], which would imply that alumina should usually act as an n-type semiconductor (unless preferential trapping by impurities causes a much higher concentration of holes compared to electrons). This agreement indicates that the semiconductor work function concepts could be applicable for alumina. In situ dielectric property measurements on fission reactor irradiated alumina have also found that alumina can be modeled as a wide-band gap semiconductor [23].

Since there are no elements with work functions less than ∼2 eV, ohmic behavior would in principle not be expected for alumina specimens with any type of electrode unless the specimen could be converted into p-type. One complication is that the ohmic or non-ohmic behavior could be affected by mechanical deformation of the specimen surface [19]. Therefore, it may not be possible to predict whether or not ohmic behavior will be observed in alumina for a given electrode material. The *I–V* characteristics can also be influenced by the gas which was used to control the specimen temperatures. The detailed analysis of the gas effect on the HFIR specimen *I–V* characteristics is described elsewhere [18]. Additional *I–V* measurements on single crystal alumina using other electrode materials are planned for the near future in order to further investigate the mechanism of ohmic and non-ohmic *I–V* behavior in alumina.

5. Summary and conclusions

In the present study, in situ measurements of the electrical conductivity and current–voltage (*I–V*) characteristics were performed both in the HFIR fission reactor with or without neutron irradiation and in a High Voltage Electron Microscope (HVEM) with or without 1 MeV electron irradiation. The results obtained are summarized as follows.

(i) RIC was observed under neutron and electron irradiation but no RIED was observed with neutron and electron irradiation up to >2 dpa and 9.1×10^{-5} dpa, respectively.

(ii) Non-ohmic current–voltage (*I–V*) characteristics were observed in alumina with or without neutron and electron irradiation.

(iii) The reason for non-ohmic behavior may be the difference of work functions between the electrode and the specimen material. This analysis suggests that alumina can be modeled as an n-type semiconductor both

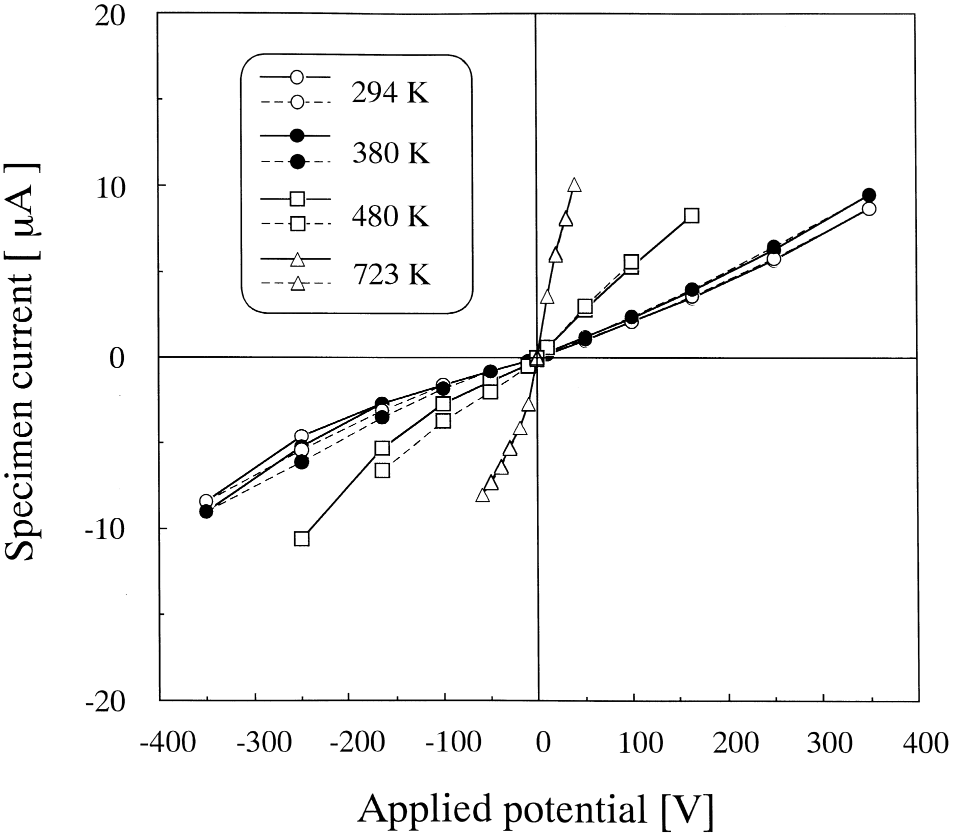

Fig. 6. Current–voltage plot of Kyocera "SA-100" single crystal alumina under irradiation with 1 MeV electron flux of 1.5 × 10^{18} e/m^2s at various temperatures. Solid and dotted lines correspond to the increasing and decreasing voltage process, respectively.

with and without irradiation. However, further *I–V* measurements are needed to confirm the mechanism of ohmic or non-ohmic *I–V* characteristic of alumina.

Acknowledgements

This study was supported by JUPITER (Japan–USA program of Irradiation Test for Fusion Research) program sponsored by the Ministry of Education, Science and Culture of Japan, and was sponsored in part by the Office of Fusion Energy Sciences, US Department of Energy under contract DE-AC05-96OR22464 with Lockheed Martin Energy Research Corp. The authors thank W.S. Eatherly for preparation of the HFIR subcapsules.

References

[1] F.W. Clinard Jr., J. Nucl. Mater. 85&86 (1979) 393.
[2] J.L. Scott, F.W. Clinard Jr., F.W. Wiffen, J. Nucl. Mater. 133/134 (1985) 156.
[3] M.M.R. Howlader, C. Kinoshita, T. Izu, K. Shiiyama, M. Kutsuwada, J. Nucl. Mater. 239 (1996) 245.
[4] C. Kinoshita, S.J. Zinkle, J. Nucl. Mater. 233–237 (1996) 100.
[5] E.R. Hodgson, J. Nucl. Mater. 179–181 (1991) 383.
[6] E.R. Hodgson, Nucl. Instr. and Meth. B 65 (1992) 298.
[7] X.-F. Zong, C.-F. Shen, S. Liu, Z.-C. Wu, Y. Chen, B.D. Evans, R. Gonzalez, C.H. Sellers, Phys. Rev. B 49 (1994) 15514.
[8] K. Shiiyama, T. Izu, C. Kinoshita, M. Kutsuwada, J. Nucl. Mater. 233–237 (1996) 1332.
[9] G.P. Pells, J. Nucl. Mater. 184 (1991) 177.
[10] J.D. Hunn, R.E. Stoller, S.J. Zinkle, J. Nucl. Mater. 219 (1995) 169.
[11] C. Patuwathavithane, W.Y. Wu, R.H. Zee, J. Nucl. Mater. 225 (1995) 328.
[12] T. Shikama, M. Narui, Y. Endo, T. Sagawa, H. Kayano, J. Nucl. Mater. 191–194 (1992) 575.
[13] L.L. Snead, D.P. White, S.J. Zinkle, J. Nucl. Mater. 226 (1995) 58.
[14] E.H. Farnum, T. Shikama, M. Narui, T. Sagawa, K. Scarborough, J. Nucl. Mater. 228 (1996) 117.
[15] W. Kesternich, F. Scheuermann, S.J. Zinkle, J. Nucl. Mater. 219 (1995) 190.

[16] W.S. Eatherly D.W. Heatherly, M.T. Hurst, A.L. Qualls, D.G. Raby, R.G. Sitterson, L.L. Snead, K.R. Thoms, R.L. Wallace, D.P. White, S.J. Zinkle, E.H. Farnum, K. Scarborough, K. Shiiyama, T. Sagawa, M. Narui, T. Shikama, in: Fusion Materials Semiannual Progress Report for Period ending 31 December 1995, DOE/ER-0313/19, Oak Ridge National Laboratory, 1995, p. 241.

[17] K. Shiiyama, C. Kinoshita, H. Suzuki, T. Izu, M. Kutsuwada, S. Matsumura, Nucl. Instr. and Meth. B 91 (1994) 284.

[18] S.J. Zinkle, W.S. Eatherly, L.L. Snead, T. Shikama, K. Shiiyama, in: Fusion Materials Semiannual Progress Report for Period ending 30 June 1997, DOE/ER-0313/22, Oak Ridge National Laboratory, 1997, p. 188.

[19] R.H. Bube, Photoconductivity of Solids, Wiley, New York, 1960, p. 110.

[20] P. Odier, J.C. Rifflet, J.P. Loup, J. Mater. Sci. 19 (1984) 2121.

[21] H.B. Michaelson, J. Appl. Phys. 48 (1977) 4729.

[22] R.C. Hughes, Phys. Rev. B 19 (1979) 5318.

[23] R.H. Goulding, S.J. Zinkle, D.A. Rasmussen, R.E. Stoller, J. Appl. Phys. 79 (1996) 2920.